Soria-Verdugo, A., Von Berg, L., Serrano, D., Hochenauer, C., Scharler, R., and Anca-Couce, A. (2019). Effect of bed material density on the performance of steam gasification of biomass in bubbling fluidized beds. *Fuel*, 257, 116118.

DOI: https://doi.org/10.1016/j.fuel.2019.116118

Effect of bed material density on the performance of steam gasification of biomass in bubbling fluidized beds

Antonio Soria-Verdugo[a]*, Lukas Von Berg[b], Daniel Serrano[a], Christoph Hochenauer[b], Robert Scharler[b], Andrés Anca-Couce[b]

[a] *Carlos III University of Madrid, Energy Systems Engineering Group, Thermal and Fluids Engineering Department. Avda. de la Universidad 30, 28911, Leganés (Madrid, Spain).*

[b] *Technische Universität Graz, Institute of Thermal Engineering. Inffeldgasse 25/B, 8010, Graz (Austria).*

** corresponding author: asoria@ing.uc3m.es Tel.: +34916248465.*

Abstract

Steam gasification of lignocellulosic biomass in a bubbling fluidized bed reactor was analyzed by means of the composition of the producer gas, including tars, and temperature distribution in the reactor. The catalytic and sorbent effect of sepiolite particles was studied by comparison of the tars generated with those produced in a bed of olivine, widely used in biomass gasification applications. Sepiolite has a lower particle density, which influences the forces acting on fuel and char particles and leads to a more homogeneous distribution of them in the dense bed during the gasification process. Fluidized beds of sepiolite particles contribute to increase the heating value of the producer gas and its hydrogen content compared to gasification under the same operating conditions in olivine beds. Furthermore, the tar yield is around 25% lower when gasifying in sepiolite beds, reducing the requirement of secondary methods for tars removal. Long-term gasification tests were also conducted in a sepiolite bed to evaluate the mitigation of the sorbent/catalytic effect of sepiolite with time.

***Keywords*:** Biomass steam gasification, Fluidized bed, Olivine, Sepiolite, Tars.

Nomenclature:

CC Carbon conversion [%].

ChC Char conversion [%].

CGE Cold gas efficiency [%].

d Particle diameter [μm].

d_m Mean particle diameter [μm].

d_σ Standard deviation of the particle diameter [μm].

g Gravity acceleration [m s^{-2}].

LHV_{bio} Lower heating value of the feedstock [MJ/kg].

LHV_{gas} Lower heating value of the dry producer gas [MJ/Nm^3].

$\dot{m}_{bio}$ Mass flow rate of biomass supplied [kg s^{-1}].

$\dot{m}_{Cgas}$ Mass flow rate of carbon in the dry producer gas [kg s^{-1}].

MW Molecular weight [kg mol^{-1}].

Nm^3 Cubic meter at 20 °C and 101.325 kPa [m^3].

p Reactor pressure [bar].

$\dot{q}_{gas}$ Volumetric flow rate of dry producer gas [MJ/Nm^3].

RT Retention time [min].

t Time [min].

T Temperature [ºC].

T_{BB} Temperature at the bottom of the bed [ºC].

T_{FB} Temperature at the freeboard [ºC].

T_{TB} Temperature at the top of the bed [ºC].

U Steam superficial velocity in the bed [cm s^{-1}].

U_{mf} Minimum fluidization velocity of the bed material [cm s^{-1}].

U/U_{mf} Dimensionless steam velocity [–].

X Concentration of permanent gas species [%].

X_C Concentration of carbon in the feedstock [%].

X_{C_char} Char yield of the feedstock multiplied by the carbon content of char [%].

Greek letters:

ε Void fraction of the bed material [–].

μ_g Dynamic viscosity of the fluidizing agent [Pa s].

ρ_b Bulk density [kg m^{-3}].

ρ_g Density of the fluidizing agent [kg m^{-3}].

ρ_p Particle density [kg m^{-3}].

σ Steam-fuel equivalence ratio [–].

ϕ Sphericity of the bed material particles [–].

Abbreviations:

GC Gas Chromatograph.

HHV Higher Heating Value.

LHV Lower Heating Value.

MS Mass Spectrometer.

PSD Particle Size Distribution.

TGA Thermogravimetric Analyzer.

1. Introduction

The depletion of fossil fuels and the environmental problems derived from their use for electric power generation and transportation inspire the search for alternative energy sources to produce electricity and renewable fuels. In this sense, renewable energies are considered the best option, since they can contribute to generate clean electricity and fuels. However, their availability strongly fluctuates for most of them, as for wind or solar energy, both thermoelectric and photovoltaic. Among the different renewable energies, biomass enables a stable electricity generation and a proper availability, as well as the production of biofuels, provided that the feedstock supply is guaranteed.

Biomass can be converted by several thermochemical conversion processes, such as combustion, gasification and pyrolysis, depending on the targeted products. Biomass combustion provides useful heat, whereas a gaseous or a liquid fuel can be obtained from gasification and pyrolysis, respectively. Specifically, biomass gasification reactors can be built at industrial scales, providing a gaseous fuel characterized by a large heating value. Biomass gasifiers can be classified into autothermal and allothermal systems. Autothermal gasifiers use air or oxygen as gasification agent, producing the required heat-of-reaction by means of exothermal oxidation reactions occurring inside the gasifier [1]. In contrast, in allothermal gasifiers, an oxygen free gas, e.g., steam, is employed as gasification agent and, thus, the heat-of-reaction for gasification should be supplied externally [2], for example from the combustion of the char produced in the allothermal gasifier. Despite the fact of being an allothermal gasification process, steam biomass gasification has the potential of generating syngas with a high hydrogen content and heating value comparable

to that of oxygen blown gasifiers, avoiding the cost of an air separation unit [3]. This high hydrogen content of the generated syngas can sustain a clean [4] and energetic [5] combustion process or be employed for the production of biofuels. However, one of the main limitations for the industrial development of biomass gasification is the high tars content of the producer gas generated [6]. Therefore, a great effort is currently devoted to design effective tar removal systems. These cleaning systems can be primary methods, if tars removal occurs inside the gasifier, or secondary methods, if tars are removed from the syngas flow [7]. Besides, a low carbon conversion can be obtained in fluidized beds due to the limited temperatures, which should be hindered [8].

Fluidized bed reactors have several advantages to hold biomass gasification reactions [9]. These reactors are characterized by high thermal inertia, proper heat and mass transfer rates, and adequate mixing rates, permitting the conversion of even low-quality fuels, and allowing the scaling-up of the process [10]. In the case of allothermal gasification, dual fluidized bed gasifiers can be built using one of them to hold the biomass steam gasification reactions and the other one to burn the char produced to supply the required heat-of-reaction to the gasifier [11]. Axial mixing of fuel particles in fluidized bed reactors depends on the relation between the fuel particle density and the density of the dense bed. Fuel particles with a lower density than the dense bed, called flotsam, are more prone to be found close to the bed surface, whereas fuel particles denser than the bed, named jetsam, are more probably located close to the distributor [12,13]. In contrast, fuel particles with a similar density to the dense bed, typically known as neutrally-buoyant, circulate throughout the whole bed height. Nevertheless, the vigorous fluidization produced when increasing the gas

velocity may induce the circulation of flotsam and jetsam particles throughout the whole bed [14,15].

Concerning tars removal, fluidized beds allow the use of both primary and secondary methods. Different kind of particles can be used as bed material for fluidized bed reactors, including sorbent and catalytic materials capable of reducing the tars content of the producer gas generated [16]. Olivine is a well know catalyst for in situ tar reduction in fluidized bed gasifiers. Numerous authors have found a reduction of the tar content and an increase of the H_2 production during biomass steam gasification due to an improvement of the steam reforming and water-gas shift reaction in olivine fluidized beds compared to inert beds of silica sand [17, 18, 19]. However, Marinkovic et al. [19] found that the catalytic effect of olivine for heavy tar components is lower than for light tar components, a result in agreement with the conclusions obtained by Devi et al. [20] from the analysis of catalytic biomass tars decomposition using untreated olivine. Świerczyński et al. [21] attributed the catalytic activity of olivine to its iron content. Several methods to improve the catalytic capability of olivine have been proposed in the literature, including olivine calcination [22], wet impregnation of calcined olivine with nickel nitrate [18] and loading with active metals, such as Fe, Ni, Co, Ce, etc [23]. In the case of sepiolite, different studies have proven the tar sorption and tar cracking reactions induced by this material during biomass pyrolysis and gasification processes [24-29]. Serrano et al. [29] found an increase of the performance of a bubbling fluidized bed air gasifier working with lignocellulosic biomass when using sepiolite instead of silica sand as bed material, due to the tar reduction and mitigation of agglomeration problems in the sepiolite bed.

Biomass char has also a catalytic effect for tar removal [30,31,32]. Fuentes-Cano et al. [30] proposed a physical mechanism for tar removal by biomass char particles. In the first step, tars are absorbed by the structure of char and they are subjected to polymerization and dehydrogenation reactions, producing hydrogen and coke, which is accumulated on the biomass char [33]. Coke can also be further converted into carbon monoxide and hydrogen in the presence of steam, thus, the rate of accumulation of coke on the char surface depends on the rate of coke generation from the reaction of tars and the rate of coke consumption due to its reaction with steam. Therefore, high coke consumption rates, which can be attained by high steam partial pressure in the reactor, promote the catalytic effect of biomass char for tars removal [6].

This work is focused on studying the allothermal gasification of lignocellulosic biomass in a bubbling fluidized bed reactor using steam as gasification agent. Gasification tests were conducted using two different bed materials with catalytic/sorbent effect for tars removal, namely sepiolite and olivine, permitting also the evaluation of the effect of buoyancy forces acting over fuel particles on the gasification process, defining these “virtual buoyancy forces” as the tendency of fuel and char particles to float or sink in the dense bed. Sepiolite has a lower particle density, which can enhance the gasification performance in fluidized beds, compared to olivine, which is the most commonly used bed material for steam gasification [3]. Different steam velocities were tested for each bed material, analyzing for each operating condition the composition of the producer gas generated and the yield and composition of the tars produced during the biomass gasification process. Furthermore, to determine the sorbent

and/or catalytic effect of sepiolite, long-term tests were also run to quantify the mitigation with time of the tar removal capability of this bed material.

2. Materials and methods

2.1. Experimental setup

The experimental facility is a cylindrical lab-scale bubbling fluidized bed reactor which was previously utilized to investigate downstream the desulfurization of a real producer gas using a ZnO-adsorbent [34]. The reactor is made of stainless steel with an inner diameter of 80 mm at the bottom, which is maintained constant up to a height of 150 mm over the distributor. The reactor is wider in the freeboard, where the inner diameter is 250 mm, to reduce the gas velocity and prevent the entrainment of bed material in the gas line. The fixed bed height was 130 mm for all the gasification tests, independently of the bed material employed. The reactor is installed inside an electric oven capable of supplying a thermal power of 4 kW to the reactor wall. Figure 1 shows a schematic of the experimental setup. A commercial steam generator was used to produce a stable flow rate of steam, measured and regulated by a mass flow controller. The feeding system is composed of a hopper to store the biomass and a screw feeder to control the pellets supplied to the bed. A constant nitrogen flow rate of 0.15 kg/h was used to maintain an inert atmosphere in the whole feeding system. The reactor pressure was maintained at 2 bar during all the gasification tests by a pressure regulator. The gas released during the gasification process was circulated through a hot filter to remove solid particles. A fraction of the gas released was pumped through a condensation system built following the tar protocol, whereas the rest of the gas released was circulated to

the chimney after being subjected to a combustion process in a pilot flame. The flow rate of producer gas obtained after the condensation system was measured by a gas flowmeter prior to determine its composition in an online permanent gas analyzer ABB AO2020. Finally, the producer gas at the outlet of the permanent gas analyzer was also conducted to the chimney through the pilot flame to burn all the combustible species.

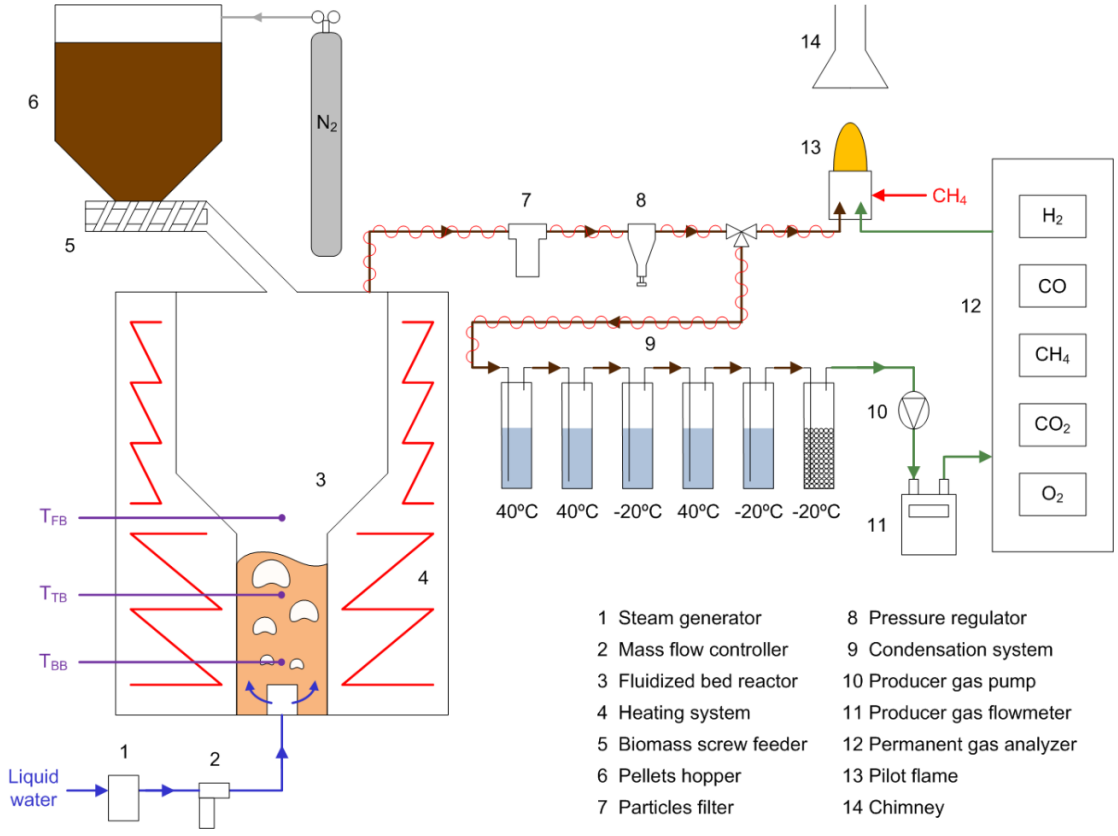

Figure 1. Schematic of the experimental setup.

2.1.2. Bed material

Olivine and sepiolite particles were used as bed material during the gasification experiments to analyze the effects of buoyancy forces of the biomass pellets on the gasification performance. The main difference between both materials is their particle density, ρ_p, which is much smaller for the sepiolite. The bulk

density, ρ_b, of both materials was also measured to calculate the void fraction, ε, of each mineral. The results of the particle and bulk densities and the void fraction of the olivine and sepiolite particles are reported in Table 1.

Table 1. Characteristics of the bed material particles.

	ρ_p [kg/m^3]	ρ_b [kg/m^3]	ε [-]
Olivine	3300	1481.2	0.55
Sepiolite	1550	812.5	0.48

The particle size distribution (PSD) of both bed materials was measured using a sieve shaker Retsch AS 200. Sieves with apertures of 53, 106, 180, 250, 425, and 600 μm were assembled on the sieve shaker. A mass above 300 g of each sample was sieved and the percentage of mass retained on each sieve was measured. The results obtained for the PSD of olivine and sepiolite particles are depicted in Figure 2, together with a Gaussian fitting of the data for both materials. In both cases, the Gaussian fitting is in good agreement with the measured PSD, obtaining a mean value, d_m, of 260 μm for olivine and 240 μm for sepiolite, and a standard deviation, d_σ, of 55 and 40 μm, for olivine and sepiolite, respectively. Therefore, a similar PSD was employed for the olivine and sepiolite particles.

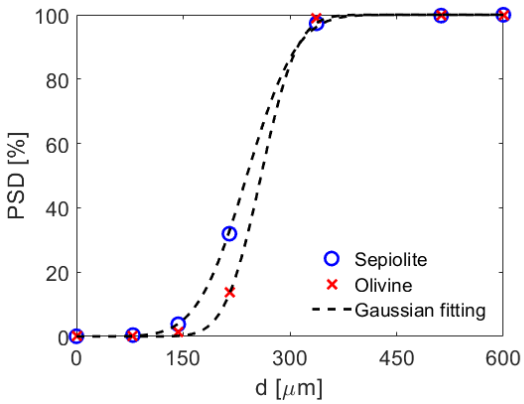

Figure 2. Particle size distribution of olivine and sepiolite.

2.2. Biomass characterization

The biomass supplied to the reactor was wood pellets of 6 mm in diameter and a regular length around 3 times the diameter. The biomass was characterized prior to the gasification tests by means of a proximate analysis, an ultimate analysis, a higher heating value test, and a particle density measurement. The proximate analysis was carried out in a TGA Q500 from TA Instruments, where the moisture and volatile matter contents were determined in a heating test under an inert atmosphere and the ash content was measured as the residue after the complete combustion of the sample. The ultimate analysis was performed in a TruSpec CHN Macro and a TruSpec S analyzer from Leco, in which the contents of carbon, hydrogen, and sulfur were measured circulating the exhaust fumes from a complete combustion of the sample through infra-red detectors, while the nitrogen content was determined by means of a thermal conductivity cell. The higher heating value of the biomass pellets was measured in an isoperibilic calorimetric pump 6300 from Parr, where the sample was completely burned under a pure oxygen pressurized atmosphere. Finally, the particle density of the biomass pellets used as feedstock was measured using an Ohaus Discovery DV-215CD microbalance and a density kit consisting of a fridge, a fastening frame, and two suspension plates that permitted the weighting of the sample in air and immersed in water. Further details of the equipment employed for the basic characterization of biomass, including their accuracy, can be found elsewhere [35,36].

The results of the basic characterization of the wood pellets are included in Table 2. This biomass is characterized by a high content of volatile matter and reduced contents of ash, nitrogen, and sulfur. Regarding the high heating value and the particle density, the values obtained are typical values for densified wood. Considering the wood pellets density and the bulk density of olivine and sepiolite (see Table 1), the biomass particles will suffer ascending buoyancy forces in the olivine bed, in which these pellets behave as flotsam particles, and they will be more probably located close to the bed surface. In contrast, descending buoyancy forces will appear on the wood pellets moving in the sepiolite bed, where these particles show a jetsam character, being more prone to be found at the bottom of the bed [13,37]. The effect of these two opposite buoyancy forces acting on the biomass pellets when moving in olivine or sepiolite fluidized beds can be studied by comparison of the gasification results obtained in these two beds under the same operating conditions.

Table 2. Results of the basic characterization of the biomass pellets (PA: Proximate Analysis, UA: Ultimate Analysis, M: Moisture, VM: Volatile Matter, FC: Fixed Carbon, A: Ash, C: Carbon, H: Hydrogen, N: Nitrogen, S: Sulfur, O: Oxygen, HHV: Higher Heating Value, wb: wet basis, db: dry basis, daf: dried ash free basis, * calculated by difference).

PA [%wb]				**UA [%daf]**					**HHV**	ρ_p
M	**VM**	**FC***	**A**	**C**	**H**	**N**	**S**	**O***	**[MJ/kg db]**	**[kg/m^3]**
7.0	78.8	13.9	0.3	52.0	7.2	0.1	0.1	40.6	20.44	1189.0

After the gasification of the biomass pellets, the density of the char produced is substantially lower than the density of the original biomass. The reduction of

density during pyrolysis is around 2/3. The reduction in volume due to pyrolysis shrinkage is around 54% for wood pellets [38], being of 64% for wood chips or logs [39], while the char yield is around 15% for wood pellets pyrolysis at the gasifier temperature [38]. This results in a char density lower than the dense bed density for both olivine and sepiolite beds. Thus, independently of the bed material used, the char density is expected to be lower than the density of the fluidized bed. The presence of char particles close to the bed surface will be then more probable in both the olivine and the sepiolite fluidized bed reactors. Therefore, according to the densities, the gasification of the biomass pellets in the bed of olivine particles is expected to occur close to the bed surface, where both the biomass pellets and the char particles will be located due to their lower density compared to the dense bed of olivine particles. In contrast, the heating-up, drying and pyrolysis of pellets in the sepiolite bed is expected to occur at the bottom of the bed due to the higher density of the biomass pellets compared to the bed material, while the lower density of the char particles promotes an increase of the concentration of char closed to the sepiolite bed surface, where char gasification would take place to a significant extent.

2.3. Experimental procedure

The gasification experiments in the bubbling fluidized bed reactor were conducted for fixed values of the temperature and pressure in the bed of 750 ºC and 2 bar, respectively, and for a constant biomass feeding rate of 380 g/h. This bed temperature is adequate for biomass gasification [40,41], while it is low enough to prevent sintering and agglomeration problems in the bed during operation [42]. The control system regulates the power released by the electric oven surrounding the reactor to maintain a constant temperature of the bed,

defined as the average between the temperatures at the freeboard, T_{FB}, the top of the bed, T_{TB}, and the bottom of the bed, T_{BB}. The pressure of the bed was adjusted by a pressure regulation valve and the biomass feeding rate was regulated by controlling the velocity of the biomass screw feeder located at the bottom of the pellets hopper.

Olivine and sepiolite beds were employed to hold the gasification reactions of biomass. The analysis of the results obtained for the gasification of biomass in beds of these two materials permits the evaluation of the effect of both the bed fluid-dynamics and the buoyancy effects on the gasification performance. Furthermore, the flow rate of steam supplied to the olivine and sepiolite beds was also varied to obtain in both cases values of σ = 5 and σ = 6. The steam-fuel equivalence ratio σ is defined as the ratio of actual provided steam to the amount of steam necessary for a full stoichiometric conversion of the fuel to H_2 and CO, comparable to the air-fuel-equivalence ratio λ used for combustion [34]. These values of σ correspond to the same steam velocity in the beds of olivine and sepiolite of U = 6.2 cm/s and U = 7.4 cm/s, respectively for σ = 5 and σ = 6. The steam mass flow rate required for each σ value was produced by the steam generator and adjusted by the steam mass flow controller.

The gasification experiments start by heating the bed to the desired temperature, 750 ºC in all cases. During the heating process, once the bed temperature reaches 400 ºC, the steam generator is switched on and the required steam mass flow rate for the test is supplied to the bed, so that the steam generator performance is stable when the desired bed temperature for gasification is attained. When the bed temperature reaches 750 ºC, the biomass

feeding starts, at a constant feeding rate of 380 g/h. After around 2 h from the beginning of the biomass feeding, the conditions of the reactor are stable to start the first measurement period, collecting tars and measuring the composition of the permanent gases generated. The sampling time for each measurement lasts 40 min. A second measurement was also run, 40 min after the end of the first test, for each bed material and steam mass flow rate, to check the repeatability of the results obtained. A high repeatability was attained for all the experimental conditions analyzed, thus, the results reported in next section correspond to those obtained during the second measurement period in all cases, i.e., around 3.5 h after the start of the biomass feeding. For the tests with sepiolite as bed material at gasification conditions of σ = 6, long-term tests were also conducted to investigate the possibility of a sorbent and/or catalytic effect of the sepiolite particles. The composition of the producer gas and the tar content was measured a third time after about 4.5 h to check if the capability of sepiolite to absorb tars was mitigated as time progresses.

Tars collected following the tar protocol were analyzed to determine the contents of water and different components per unit of volume of producer gas. The water content was measured directly applying the Karl Fischer technique, whereas the characterization of the tars content was carried out using the gravimetric method and measuring the contents of each species in a Gas Chromatograph – Mass Spectrometer (GC-MS). The water content of the tars collected were measured in triplicates using a Karl Fischer Titrator V30 Compact Volumetric from Mettler Toledo, obtaining deviations below 2%.

Tar samples collected using the tar protocol were analyzed both qualitatively and quantitatively by means of a Varian 431-GC coupled to a Varian 210-MS

(ion trap). Samples of 1 μl, with added tert-butylcyclohexane as internal standard, were injected at 300 ºC in split mode (1:50). The samples were circulated through a non-polar capillary column (VF-5MS) using helium as carrier gas at a constant flow rate of 1.2 ml/min. The total duration of the GC oven program was 80 min, consisting in an isothermal process for 5 min at the initial temperature of 30 ºC, a temperature increase up to 180 ºC with a constant heating rate of 2.5 ºC/min, and a final increase up to 300 ºC with a constant heating rate of 8 ºC/min. The MS was set in automatic ionization mode with a scan mode between 50 and 250 m/z mass range and a solvent delay of 2.1 min. The ion trap, manifold and transfer line were maintained at 210 ºC, 60 ºC and 300 ºC, respectively. Tars identification was carried out employing the NIST 2.0 library, while tars quantification was performed using the tert-butylcyclohexane/naphthalene calibration curve. Each sample was injected twice to check the system repeatability, obtaining average deviations below 3% for all the species detected.

3. Results and Discussion

3.1. Minimum fluidization velocity

The minimum fluidization velocity, U_{mf}, of the olivine and sepiolite particles employed as bed material during the gasification tests was measured in a lab-scale reactor with optical access through the top. The cylindrical lab-scale reactor was made of stainless steel, with an inner diameter of 4.7 cm and a height of 50 cm. The reactor was surrounded by three electric resistors capable of supplying a total thermal power of 1.5 kW to the bed. The resistors were connected to a potentiometer that controlled the thermal power released and

the bed temperature was measured by an immersed thermocouple. The fixed bed height was set to 130 mm both for olivine and sepiolite, equal to that employed in the gasification reactor. The fluidizing agent employed for the U_{mf} measurements was nitrogen. The nitrogen flow rate supplied to the bed was measured by a PFM710-C6-E flowmeter, from SMC, with a measuring range from 0.2 to 10 L/min. Further details of the facility employed for the minimum fluidization velocity measurements can be found in Soria-Verdugo et al. [43] and Morato-Godino et al. [44].

The measurement of U_{mf} as a function of the bed temperature, T, was based on the visual inspection of the bed surface. Considering the size and density of olivine and sepiolite particles, both of them are classified as type B particles according to Geldart's classification [45]. Geldart B particles are characterized by starting bubbling for a gas velocity just above the minimum fluidization velocity, i.e., the minimum fluidization velocity and the minimum bubbling velocity coincide for type B particles. Therefore, the minimum fluidization velocity was determined as the minimum velocity for which bubbles were detected at the bed surface. Furthermore, to prevent the effect of cohesive forces between particles in the bed, the minimum fluidization velocity was measured, for each temperature and bed material, reducing the gas velocity from a vigorous bubbling fluidized bed until no bubbles were detected at the bed surface.

The evolution of the minimum fluidization velocity of type B particles with temperature can be estimated using the Carman-Kozeny (C-K) correlation [46], in which the effect of temperature is accounted for by the variation of the fluidizing gas properties,

$$U_{mf} = \frac{\left(\phi\, d_m\right)^2 \left(\rho_p - \rho_g\right) g}{180 \mu_g} \frac{\varepsilon^3}{1-\varepsilon}, \quad (1)$$

where U_{mf} is the minimum fluidization velocity, ϕ is the sphericity of the solid particles, ε is the void fraction, g is the gravity acceleration, d is the particle diameter, ρ_p is the density of solid particles, and ρ_g and μ_g are the density and dynamic viscosity of the fluidizing agent, respectively.

The particle density, ρ_p, and void fraction, ε, of the solid particles reported in Table 1 were included in the C-K correlation, together with the mean diameter, d_m, obtained from the Gaussian fitting of the PSD. Then, the sphericity of the olivine and sepiolite particles, ϕ, can be obtained as a free parameter of the fitting of the experimental measurements of the minimum fluidization velocity conducted in the lab-scale reactor as a function of temperature, considering the variation of the density and dynamic viscosity of nitrogen with temperature as described in Sánchez-Prieto et al. [47]. The values obtained for the sphericity of olivine and sepiolite following this procedure are 0.61 and 0.73, respectively. Once the sphericity of the solid particles is known, the values of U_{mf} can be predicted for a different fluidizing agent and for different operating conditions.

A lower minimum fluidization velocity was obtained for the sepiolite bed compared to the olivine bed due to the slightly smaller size and significantly lower density of sepiolite. The final estimation of the minimum fluidization velocity of the solid particles fluidized by steam at 750 ºC and 2 bar is U_{mf} = 4.4 cm/s for the olivine particles and U_{mf} = 1.4 cm/s for the sepiolite particles. These values are in agreement with the measurement of U_{mf} in the gasifier using the $\Delta p - u$ curve. Therefore, the steam velocities employed to attain values of σ = 5

and σ = 6 result in a smooth fluidization of the olivine bed, corresponding to low values of the dimensionless gas velocity of U/U_{mf} = 1.4 and U/U_{mf} = 1.7, respectively. In contrast, the fluidization in the sepiolite bed under the same operating conditions is vigorous, obtaining dimensionless gas velocities in this case of U/U_{mf} = 4.4 and U/U_{mf} = 5.3, respectively for the σ = 5 and σ = 6 tests.

The smooth fluidization in the bed of olivine particles promotes the segregation of both biomass pellets and char particles to the bed surface, due to their lower density compared to the olivine dense bed [14,15]. However, the large bubbles present in the sepiolite bed due to a vigorous fluidization enhance the axial mixing inside the bed, which induces a more homogeneous distribution of flotsam (char particles) and jetsam (biomass pellets) particles throughout the whole bed height [13].

3.2. Temperature distribution inside the bed

The reactor temperature was monitored during the gasification experiments using three thermocouples. Two of the thermocouples were immersed in the bed, one of them at the bottom of the bed, T_{BB}, and the other close to the bed surface, T_{TB}, whereas the third thermocouple was located at the freeboard, T_{FB}. The control system adjusts the thermal power released by the furnace to keep the average of these three temperatures close to the set point, which in this study is 750 ºC. Therefore, provided that the control system operates accurately, the average of these three temperatures will be 750 ºC in all cases, however, the values of each temperature may differ depending on the operating conditions of the gasification process. Specifically, the endothermic character of the reactions and processes taking place in the gasifier (heating-up, drying,

pyrolysis, and char gasification) might promote a reduction of the temperature in the zone of the bed where the biomass particles are more prone to be located, which will be strongly influenced by buoyancy effects on the biomass particles.

Table 3 shows the mean and standard deviation of the three reactor temperatures during the gasification tests in the olivine and sepiolite beds, fluidized by steam under σ = 5 and σ = 6. In all cases, the average of the three temperatures is close to 750 ºC, which proves the accuracy of the temperature control system. The variability of the temperature measurement is higher, i.e., higher standard deviation, for the freeboard temperature in both beds, since the dense beds provide a higher thermal inertia in this zone of the reactor compared to the freeboard. Furthermore, the standard deviations of temperature in the bed of sepiolite particles, e.g., for the bottom and top temperatures, are higher than those of the olivine bed, due to the lower thermal inertia of the sepiolite bed caused by the lower density of these particles compared to olivine (see Table 1).

Table 3. Mean and standard deviation of the temperature at the bottom of the bed (T_{BB}), close to the bed surface – top of the bed (T_{TB}) and freeboard (T_{FB}) during the measurement period.

	Olivine		**Sepiolite**	
	σ = 5	**σ = 6**	**σ = 5**	**σ = 6**
T_{BB} [ºC]	749.2 ± 0.6	738.9 ± 0.6	733 ± 2	740 ± 3
T_{TB} [ºC]	728.0 ± 1.0	725.7 ± 0.8	755 ± 3	749 ± 9
T_{FB} [ºC]	773 ± 5	786 ± 5	764 ± 9	762 ± 9

In the olivine bed, the lower temperature of the reactor during biomass gasification was found at the top of the bed, T_{TB}. In this fluidized bed, the high

density of olivine particles promotes the appearance of ascending buoyancy forces on the biomass pellets, which are lighter than the olivine bed, limiting their movement to a restricted zone close to the bed surface. Furthermore, the segregation of biomass pellets in the olivine bed is promoted by the smooth fluidization produced for the values of σ tested, corresponding to dimensionless gas velocities of only U/U_{mf} = 1.4 for σ = 5 and U/U_{mf} = 1.7 for σ = 6. Therefore, the reduced temperature at the top of the reactor might be attributed to the endothermic character of the reactions and processes to which the biomass pellets are subjected in this zone of the bed. Comparing the values of the reactor temperatures in the bed of olivine for the gasification tests of σ = 5 and σ = 6, a reduction of the temperature at the bottom of the bed, T_{BB}, is observed in the tests conducted at σ = 6. In this case, the higher steam velocity results in greater bubbles inside the bed, capable of inducing the circulation of some of the biomass pellets throughout the bed [14,15], thus, the gasification of some of the biomass pellets may occur at the bottom of the bed for σ = 6, resulting in a slight reduction of temperature in this zone of the reactor.

In contrast to the results in the olivine bed, the temperature distribution during biomass gasification in the bed of sepiolite particles is quite different. The lowest temperature of the sepiolite bed during the gasification test at σ = 5 is the temperature at the bottom of the bed, instead of the temperature at the top of the bed as in the olivine bed. In this case, the lower density of the sepiolite bed compared to the biomass pellets promotes the jetsam character of the fuel particles, which will be more probably located at the bottom of the bed due to descending buoyancy forces [44]. Therefore, the endothermic processes in the gasifier occur primarily at the bottom of the sepiolite bed, causing a decrease of

temperature in this zone of the reactor. However, the vigorous fluidization of the sepiolite bed during the gasification at σ = 6, which corresponds to a high dimensionless gas velocity of U/U_{mf} = 5.3, enhances the axial mixing of even strongly jetsam particles [13], increasing the homogeneity in the distribution of the biomass particles throughout the whole bed height, which leads to similar temperatures at bottom and top of the bed during these tests.

3.3. Producer gas composition

The composition of the producer gas, obtained after the tars condensation system, was determined measuring the concentration of H_2, CO, CO_2, CH_4, and O_2 by a permanent gas analyzer, obtaining the concentration of N_2 by difference. At the beginning of each sampling, the line contains air, thus the concentration of H_2, CO, CO_2, and CH_4 are null. As the sampling progresses, the concentration of these permanent gas species increases to reach a constant value, whereas the concentration of O_2 is reduced to zero and the concentration of N_2 (obtained by difference) decreases to a constant value due to the nitrogen flow rate supplied to the biomass feeding system to guarantee an inert atmosphere in this zone of the reactor. This N_2 flow rate was fixed to the same constant value for all the cases analyzed.

The time evolution of the permanent gasses' volumetric concentration in a dry basis during the gasification tests in the beds of olivine and sepiolite, operating with values of σ = 5 and σ = 6, are depicted in Figure 3. The tendency of the curves is similar in all the gasification tests conducted, attaining steady values for the concentration of the different permanent gases analyzed after approximately 10 min. This shows that the gasifier was operated at stable

conditions. In all cases, the concentration of oxygen decreases rapidly to zero when the air contained in the measuring line (the gasification test started long before the measurement, as stated in Section 2) is displaced by the producer gas, guaranteeing the air tightness of the tar condensation system and the producer gas line.

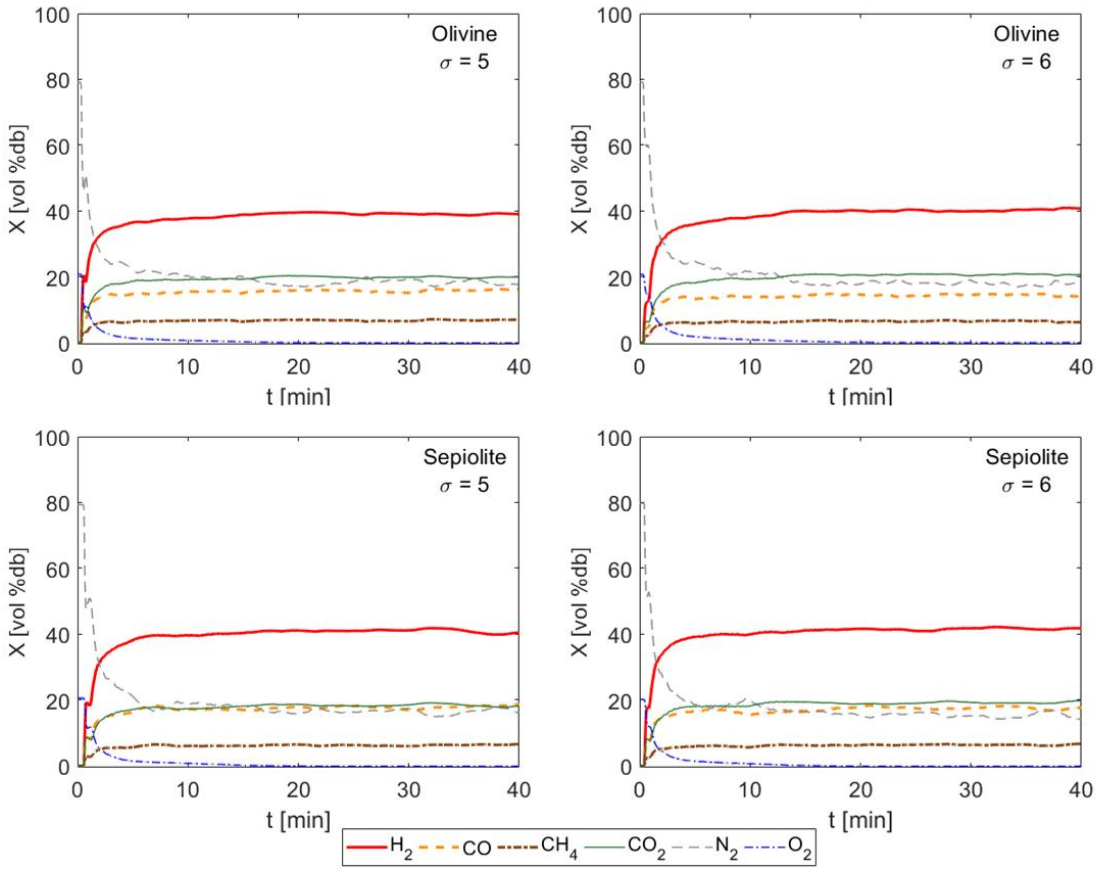

Figure 3. Time evolution of the producer gas composition (Note: the initial O_2 concentration is from air in the measuring line which is displace by the producer gas when the measurement starts, dropping its concentration to zero).

The constant concentration attained by the different species, defined as the average value during the last 20 min in Figure 3, are included in Table 4 to facilitate the comparison of the results between different cases. Both for the olivine and the sepiolite beds, the increase of the σ value results in an increase

of the concentration of H_2 in the producer gas due to the higher amount of steam available in the reactor [49]. The effect of varying σ on the concentration of CH_4 is slight in both beds, with a reduction with higher σ values. The concentration of CO is also reduced when increasing the value of σ during gasification, especially in the case with a fluidized bed of olivine particles. Regarding CO_2, its concentration in the producer gas is augmented when increasing σ, independently of the type of particles conforming the fluidized bed, whereas the opposite effect is observed for the concentration of N_2. The results reported in Table 4 for the volumetric concentration of the different permanent gases are comparable to those obtained by Schweitzer et al. [50] from the steam gasification of wood pellets at 800 ºC in a dual fluidized bed, although a higher concentration of H_2 was attained in our facility. The volumetric concentration of the different components of the producer gas obtained in this work are also similar to those reported by Kraussler et al. [51] for the steam gasification of wood chips in a dual fluidized bed at 850 ºC.

The effect of the bed material on the producer gas composition is also significant. The concentrations of H_2 and CO are higher in the sepiolite bed by 1.8% – 2.1 % and 2.0% – 2.7%, respectively, while the concentration of CH_4 is slightly reduced by 0.4% – 0.5% in the bed of sepiolite particles. Therefore, the heating value of the producer gas obtained from the gasification of biomass in a sepiolite bed is higher than that generated in a bed of olivine particles, as shown in Table 4, where the lower heating value (LHV) of the producer gas was calculated from the composition according to Basu [52] and at normal conditions (20°C, 1 bar). The effect of the σ value on the LHV of the producer gas is slight for both bed materials. This result is in agreement with the work of

Karatas and Akgun [53], who found that the producer gas LHV was hardly affected by the steam to biomass ratio during steam gasification of walnut and pistachio shells in a bubbling fluidized bed.

Concerning the non-combustible components of the producer gas, the concentrations obtained for CO_2 and N_2 are lower in the sepiolite bed by 1.5% – 1.7% and 1.8% – 2.7%, respectively. In particular, the lower value obtained for the concentration of N_2 in the sepiolite bed informs of a larger generation of producer gas in this case, since the N_2 flow rate used to guarantee an inert atmosphere in the feeding system is constant for all the gasification tests. This higher generation of producer gas might be attributed to two different factors: a higher gasification conversion due to a faster and more homogeneous heating of the biomass pellets [54] or a higher effect of the interaction between tars and char [6]. The heating is faster in the bed of sepiolite particles, where the biomass pellets are immersed in the dense bed due to the descending buoyancy forces, in contrast to the olivine bed, where the lower density of the pellets compared to the bed and the smooth fluidization promotes ascending buoyancy forces on the biomass pellets, inducing the biomass particles to segregate to the bed surface, where the heating of the particles is less efficient and actually lower temperatures are obtained (see T_{TB} for olivine particles in Table 3). In addition, the possible interaction between tars and char is also higher in the sepiolite bed, where a more homogeneous distribution of biomass pellets and char particles in the whole bed is expected due to the vigorous fluidization in this case. However, the smooth fluidization and the lower density of both biomass pellets and char particles compared to the olivine dense bed, induced an increase of the concentration of biomass and char close to the bed

surface, preventing the interaction between tars generated during the biomass gasification in this zone and char particles, because of the limited residence time of tars, which are released close to the olivine bed surface. In contrast, tars are released at the bottom of the sepiolite bed, or at least inside the dense bed if the fluidization is vigorous enough, increasing the residence time of tars and the possibility of interaction with the catalytic char particles.

Table 4. Average concentration of the different species in the producer gas during the last 20 min of the gasification test and lower heating value (Note: the concentration of O_2 is zero in all cases).

	Olivine		**Sepiolite**	
	σ = 5	**σ = 6**	**σ = 5**	**σ = 6**
H_2 [vol %db]	39.2	40.2	41.0	42.3
CO [vol %db]	15.8	14.6	17.8	17.3
CH_4 [vol %db]	6.8	6.5	6.3	6.1
CO_2 [vol %db]	19.9	20.7	18.4	19.0
N_2 [vol %db]	18.3	18.0	16.5	15.3
LHV [MJ/Nm^3]	8.08	7.94	8.33	8.32

3.4. Gasification efficiency and conversion

The cold gas efficiency (*CGE*), carbon conversion (*CC*) and char conversion (*ChC*) were determined for each gasification test conducted. The *CGE* was calculated as the ratio of energy contained in the producer gas to the energy supplied by the fresh biomass [52]:

$$CGE = \frac{LHV_{gas} \cdot \dot{q}_{gas}}{\dot{m}_{bio} \cdot LHV_{bio}}, \quad (2)$$

where LHV_{gas} is the lower heating value of the dry producer gas, $\dot{q}_{gas}$ is the volumetric flow rate of dry producer gas, $\dot{m}_{bio}$ is the mass flow rate of biomass pellets supplied to the gasifier and LHV_{bio} is the lower heating value of the feedstock. For the calculation, the volumetric flow rate of producer gas $\dot{q}_{gas}$ was determined from a mass balance of the nitrogen flow.

The *CC* was computed as the ratio of carbon contained in the dry producer gas, in the form of CO, CO_2, and CH_4, to the carbon supplied by the biomass pellets [52]:

$$CC = \frac{MW_C}{\dot{m}_{bio} \cdot X_C} \left(\frac{\dot{m}_{CO}}{MW_{CO}} + \frac{\dot{m}_{CO_2}}{MW_{CO_2}} + \frac{\dot{m}_{CH_4}}{MW_{CH_4}} \right), \quad (3)$$

where X_C is the carbon content of the feedstock and MW_j and $\dot{m}_j$ are the molecular weight and mass flow rate of the component *j*, respectively.

The char conversion was determined considering the mass flow rate of carbon and char supplied to the gasifier, and the mass flow rate of carbon in the producer gas:

$$ChC = 1 - \frac{\dot{m}_{bio} \cdot X_C - \dot{m}_{Cgas}}{\dot{m}_{bio} \cdot X_{C\_char}}, \quad (4)$$

where X_{C_char} is the char yield from pyrolysis of the feedstock multiplied by the carbon content of char and $\dot{m}_{Cgas}$ is the carbon mass flow rate of the producer gas. A char yield of 15% in a dry basis and carbon content in the char of 92% has been assumed for this case, based on literature results of pyrolysis experiments with wood pellets conducted at 750°C [38].

The results obtained for the cold gas efficiency (*CGE*), carbon conversion (*CC*) and char conversion (*ChC*) of each gasification test are included in Table 5. In the olivine bed, no effect of the σ value was found on the *CGE*, *CC* or *ChC*. However, higher values of *CGE*, *CC* and *ChC* were attained in the sepiolite bed, obtaining also an increase of the three parameters with σ. Regarding the *CGE*, a significant increase was obtained when increasing σ from 5 to 6 in the sepiolite bed, even though the LHV of the producer gas is unaffected by the σ value (Table 4). This result is caused by a higher gas production for σ = 6 in the sepiolite bed, which is in accordance with the lower concentration of nitrogen measured in the producer gas for this case. This higher gas production in the sepiolite bed operated at σ = 6 may be induced by a higher char conversion, as indicated by the substantial increase of *ChC* compared to the results at σ = 5 in the sepiolite bed. The char conversion is limited in the case with olivine, where most of the produced char is not converted. Char conversion is much higher with sepiolite, obtaining a value close to 100% for σ = 6. A higher char conversion also results in a higher carbon conversion, as shown in Table 5. The values of *CGE* reported in Table 5 should be carefully considered, since the furnace surrounding the reactor was heating during the tests, introducing an external energy input to the system. The average energy input during the gasification tests in the olivine bed at σ values of 5 and 6 was 2.3 and 2.5 kW, respectively, whereas in the sepiolite bed an average of 3.1 kW was supplied for σ = 5 and 3.4 kW for σ = 6. However, this energy supplied by the furnace is partly lost due to heat losses of the system and only a fraction is effectively supplied to the bed. This energy supplied to the bed from the furnace is the reason why the values of *CGE*, where no heating energy input is considered, is

even higher than 100% in some case. Nevertheless, although the values of *CGE* cannot be considered as an absolute efficiency, these values can be used to compare the results obtained for the different beds and operating conditions tested.

Table 5. Cold gas efficiency (*CGE*), carbon conversion (*CC*) and char conversion (*ChC*) obtained for each gasification test.

	Olivine		**Sepiolite**	
	σ = 5	**σ = 6**	**σ = 5**	**σ = 6**
CGE [%]	83.5	83.4	95.4	102.8
CC [%]	82.1	82.1	91.0	97.9
ChC [%]	32.5	32.6	65.2	92.2

3.5. Tars and water contents

The water contained in the 5 bottles filled with isopropanol is primarily obtained from condensation of the steam employed as fluidizing agent, although, in small quantities, it can also be derived from condensation of steam produced during the biomass gasification reactions. The mass of water per unit of volume of producer gas during the biomass gasification tests in the olivine and the sepiolite beds is reported in Table 6 for all the cases studied. For both bed materials, the water content increases with the value of σ as expected, due to the higher steam mass flow rate employed when increasing this parameter. However, comparing the water content in the released gases for the same values of σ in the fluidized beds of olivine and sepiolite particles, a notable reduction of around 15% of the water per unit of volume of producer gas is observed in the sepiolite bed. Considering that the water produced during the

biomass gasification is negligible compared to the amount of steam used as fluidizing agent, this reduction of water in the sepiolite bed for constant values of the steam mass flow rate implies an increase of the amount of producer gas generated and water consumed for gasification. Therefore, since the biomass feeding rate is constant for all the tests, an increase of the biomass char conversion by gasification is obtained in the sepiolite fluidized bed compared to the fluidized bed of olivine particles. This result is in agreement with those obtained for the estimated char conversion, with a higher conversion for sepiolite as shown in Table 5.

Table 6. Water content in the released gases after gasification per unit of volume of producer gas [g/Nm^3].

	Olivine		**Sepiolite**	
	σ = 5	**σ = 6**	**σ = 5**	**σ = 6**
H_2O	433.0	526.4	365.1	447.6

Table 7 shows the concentration of 24 tar species identified by the GC-MS for the gasification tests conducted in fluidized beds of olivine and sepiolite particles operated at σ = 5 and σ = 6, together with their retention time (*RT*) in the GC. Benzene has the highest concentration among all the tar species in all cases, with a concentration of approximately 4 g/Nm^3 for the olivine bed and around 3 g/Nm^3 for the sepiolite bed, followed by naphthalene with roughly half the concentration of benzene, and toluene with concentrations of around 0.9 and 0.45 g/Nm^3 for the olivine and sepiolite beds, respectively.

Table 7. Concentration of various tar components per unit of volume of producer gas [g/Nm^3].

Compound	RT [min]	Olivine		Sepiolite	
		$\sigma = 5$	$\sigma = 6$	$\sigma = 5$	$\sigma = 6$
Benzene	3.17	4.283	4.068	3.189	2.815
Toluene	6.33	0.967	0.842	0.489	0.418
2-Pentanone, 4-hydroxy-4-methyl-	10.67	0.040	0.009	0.037	0.065
Ethylbenzene	11.58	0.007	0.004	0.002	0.003
Xylene	12.13	0.088	0.073	0.033	0.025
Styrene	13.50	0.203	0.177	0.087	0.070
Phenol	19.78	0.284	0.225	0.128	0.133
Benzofuran	20.24	0.101	0.088	0.052	0.047
Ethylcyclohexane	22.61	0.025	0.025	0.022	0.024
Indene	23.21	0.582	0.575	0.416	0.394
Naphthalene	31.73	2.202	2.127	1.571	1.413
2-methylnaphthalene	38.00	0.159	0.128	0.067	0.056
1-methylnaphthalene	38.80	0.078	0.065	0.034	0.031
Biphenyl	42.56	0.069	0.060	0.034	0.030
Acenaphthalene	45.82	0.468	0.454	0.361	0.326
Acenaphthene	47.49	0.058	0.064	0.077	0.067
1,1'-Biphenyl, 2-methyl-	47.43	0.010	0.007	0.003	0.003
Dibenzofuran	49.19	0.150	0.146	0.133	0.134
Fluorene	52.24	0.244	0.229	0.198	0.180
Phenanthrene	60.80	0.448	0.396	0.323	0.280
Anthracene	61.34	0.079	0.075	0.052	0.050
4,5-Methylene phenanthrene	66.04	0.068	0.065	0.054	0.057
Fluoranthene	69.59	0.158	0.172	0.160	0.153
Pyrene	70.56	0.138	0.131	0.109	0.102

The amount of tars collected was also measured using the gravimetric method and compared to the results obtained from the GC-MS analysis. The results of the total amount of tars per unit of volume of producer gas obtained from both methods are reported in Table 8, for the gasification tests in the olivine and sepiolite beds at $\sigma = 5$ and $\sigma = 6$. The tar content measured by GC-MS is higher than that determined by the gravimetric method for both the olivine and sepiolite

beds, independently of the value of σ. These differences may be attributed to the volatilization of light tars compounds such as benzene, toluene, ethylbenzene, and xylenes (BTEXs) when measuring the tars content with the gravimetric method, since they are partially evaporated with the solvent [55,56]. This is likely the case here, as the tars detected by the gravimetric method roughly correspond to the tars measured by GC-MS without considering BTEXs (see Table 7). This higher concentration of tars measured by GC-MS compared to the gravimetric method was also obtained by Schweitzer et al. [50] analyzing gasification of wood pellets, in contrast to the results obtained for other dirtier biomass such as sewage sludge and cattle or pig manure.

Table 8. Tars content generated during the biomass gasification tests per unit of volume of producer gas [g/Nm^3].

	Olivine		**Sepiolite**	
	σ = 5	**σ = 6**	**σ = 5**	**σ = 6**
Gravimetric method	6.36	5.14	4.97	4.04
GC-MS	10.91	10.21	7.63	6.88

The amount of tars generated during wood pellets gasification in both the olivine and the sepiolite beds decreases when σ is increased due to the higher amount of steam available in the reactor and better fluidization. In contrast, the tar production in the sepiolite bed is lower than in the olivine bed, which, as stated above, might be caused by the longer residence time of the tars released to interact with the catalytic char, or by a sorption and/or catalytic capability of the sepiolite particles.

For an easier comparison of the results of tars content during the different tests, Figure 4 shows the concentration of tar species classified in different classes:

Benzene, class 2, class 3, class 4, and class 5. The general tendency observed in Figure 4 is a reduction of the tars content when increasing σ. Comparing the results obtained for the tars content in olivine and sepiolite beds, a general reduction of the tars generated in the sepiolite bed is also visible in Figure 4. This reduction of the tars content can be caused by the longer time available for the catalytic effect of the char produced in the sepiolite bed, confirming the conclusions attained from the results of the producer gas composition. However, the reduction of the content of tars might also be caused by a sorbent and/or catalytic effect of the sepiolite particles [29], which could absorb partially the tars generated or catalyze reactions that promote their cracking. This sorption and catalytic effect of the sepiolite particles will be discussed in the next subsection, where long-term gasification tests conducted in the sepiolite bed are analyzed.

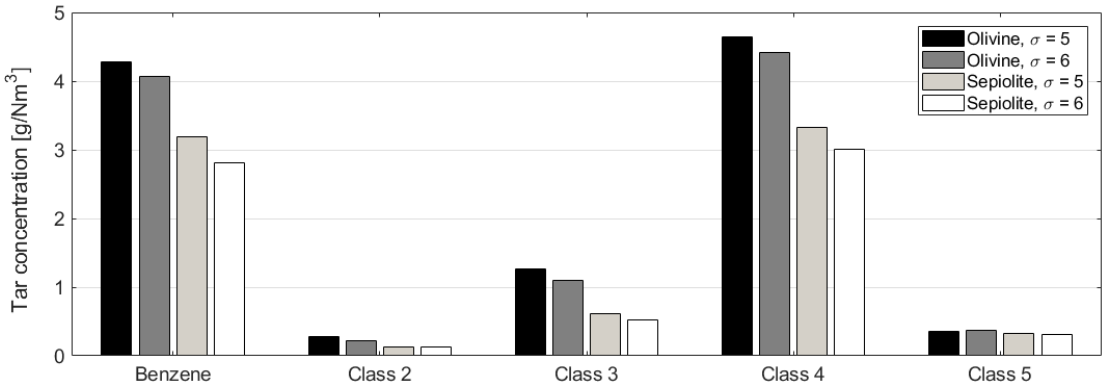

Figure 4. Tars content of different classes obtained per unit of volume of producer gas during the biomass gasification tests in olivine and sepiolite beds.

3.6. Sorption and catalytic capability of the sepiolite bed

To check if the effect of the tars reduction and increase of combustible species concentration of the producer gas during gasification in a sepiolite fluidized bed was mitigated as time progresses due to the saturation of the sepiolite sorbent

capability, long-term gasification tests were also conducted in the sepiolite bed operated at σ = 6. The tests were similar to those described above and the duration was also 40 min. However, in this case the test started around 4.5 h after the beginning of biomass feeding. The long-term test was replicated twice to check the repeatability, thus, the results reported in this section correspond to the mean and standard deviation of the two replicates.

The concentration of the different producer gas species was measured by the online permanent gas analyzer and the tars content was determined by the GC-MS. The results of the composition of the producer gas during the long-term test are included in Table 9, together with the deviations from the regular gasification test in the sepiolite bed at σ = 6, shown in Table 4. Only slight variations between the regular and the long-term tests were detected regarding the concentration of permanent gases.

Table 9. Producer gas composition during the long-term test in the sepiolite bed and deviation from the regular test at σ = 6 [%].

	H_2	CO	CH_4	CO_2	N_2
Long-term test	41.6 ± 0.3	17.6 ± 0.4	6.4 ± 0.1	19.1 ± 0.2	15.3 ± 0.6
Deviation	- 0.7 ± 0.3	0.3 ± 0.4	0.3 ± 0.1	0.1 ± 0.2	0.0 ± 0.6

Considering the concentration of the permanent gas species shown in Table 9, the resulting average lower heating value of the producer gas generated during the long-term test is 8.32 MJ/Nm^3, a similar value to that obtained for the regular gasification test at σ = 6 in the sepiolite bed (see Table 4). The average values for the cold gas efficiency, carbon conversion and char conversion during the long-term tests are 100.6, 96.7, and 87.4%, respectively. Notice that,

as stated above, the value of the cold gas efficiency is higher than 100% because the input energy supplied by the furnace is not considered in the calculation. These values are very similar, although slightly worse, to those obtained during the regular test in the sepiolite bed at σ = 6. The gasification performance during the long-term test is much better than in the olivine bed and the test with σ = 5.

The water content of the gases released during the long-term test is 453 ± 3 g/Nm^3, close to the 447.6 g/Nm^3 obtained during the regular test. In contrast, the amount of tars generated during the long-term test is slightly higher than that generated in the regular test. The tars content generated detected by the GC-MS was 7.8 ± 0.4 g/Nm^3 and by the gravimetric method was 4.6 ± 0.6 g/Nm^3 for the long-term test, which corresponds to an increment of the average tars generated compared to the regular test of 13.4% and 12.9% for the GC-MS and gravimetric method, respectively. The increase of the tars generated during the long-term test compared to the regular test occurs for all the different groups defined, as reported in Table 10.

Table 10. Comparison of tars of different classes generated during the long-term and the regular tests in the sepiolite bed at σ = 6 [g/Nm^3].

	Benzene	**Class 2**	**Class 3**	**Class 4**	**Class 5**
Long-term test	3.2 ± 0.2	0.18 ± 0.01	0.67 ± 0.04	3.33 ± 0.06	0.33 ± 0.03
Regular test	2.81	0.13	0.52	3.01	0.31

The time evolution of the temperatures measured at the freeboard, T_{FB}, the top of the bed, T_{TB}, and the bottom of the bed, T_{BB}, is shown in Figure 5 for 3 h before the end of the long-term test, including the 2 replicates conducted.

Therefore, each long-term test corresponds only to the last 40 min, as indicated in the figure. At approximately 1.5 h before the start of the long-term test, the tendency of the temperatures in the bed changed, obtaining a significant increase of the temperature at the top of the bed and a reduction of the freeboard temperature, so that, the average temperature in the reactor is maintained at 750 ºC, as established by the control system. This variation of the time evolution of temperatures may be caused by a transition of the bed hydrodynamics, motivated by the char/ash accumulation in the bed or by a change in the properties of the sepiolite particles, since all the bed operating parameters, e.g., mass flowrates, temperature set points, feeding velocity, bed pressure, etc, were kept constant. In addition, a higher variability of the temperatures is also detected after the transition, which might be the result of a change of the characteristics of bubbles in the bed. Such a change in bubbles' characteristics is an indicator of a change in the fluidized bed hydrodynamics.

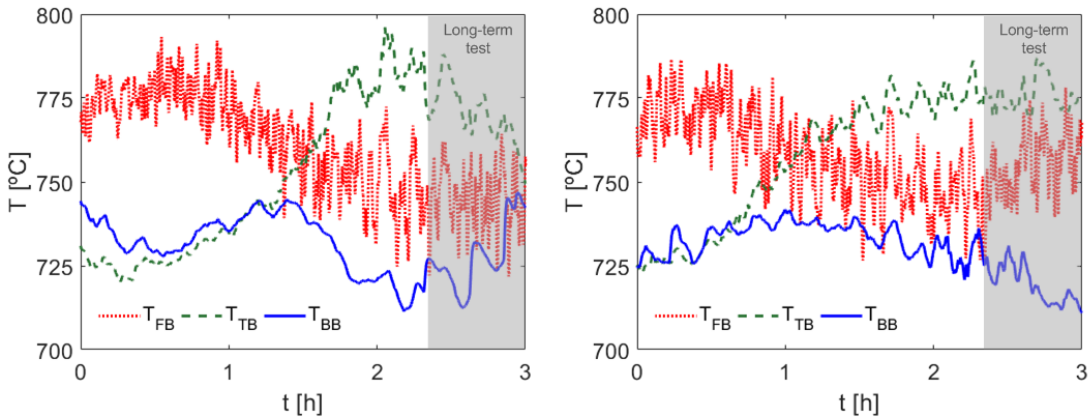

Figure 5: Time evolution of the reactor temperatures for 3 h before the end of the 2 replicates of the long-term test in the sepiolite bed operated at $\sigma = 6$.

During the long-term tests, the maximum temperature was reached at the top of the bed, whereas the minimum temperature was measured at the bottom of the

bed. In fact, the average and standard deviations obtained for each temperature during the 2 replicates of the long-term test are T_{TB} = 773 ± 7 ºC, T_{FB} = 749 ± 11 ºC and T_{BB} = 724 ± 9 ºC. This different temperature distribution may affect the tars generated. During the regular test, the highest temperature is obtained at the freeboard and, thus, the tars generated might be partially cracked when flowing through this high-temperature zone of the bed, resulting in a lower tar content of the gas released.

The slightly higher tar content during the long-term tests indicates either the mitigation of the sorption and/or catalytic effect of the sepiolite particles with time or the effect of the accumulation of char particles in the bed. Therefore, in any case, the performance of the sepiolite bed for a continuous operation would be improved by changing the bed material, i.e., removing the char particles accumulated in the bed and substituting the used sepiolite particles by fresh material. However, even operating for long time with the same sepiolite particles, the lower heating value of the producer gas is maintained, and the tar content is lower than with olivine, obtaining a higher quality and quantity of producer gas in the sepiolite bed compared to the olivine bed for the same operating conditions. Furthermore, the lower density of the sepiolite bed results in a lower pressure drop of the bed compared to the olivine case, thus, the pumping costs of the fluidizing agent are also lower in the bed of sepiolite particles.

4. Conclusions

The effect of the bed material on the steam gasification of wood pellets in a bubbling fluidized bed was studied. Sepiolite and olivine beds were tested for

various steam to biomass ratios, analyzing the composition of the producer gas and the tars generated. A larger producer gas generation, i.e., a higher conversion, was inferred for the sepiolite bed from the lower contents of water and nitrogen in the producer gas. This higher conversion in the sepiolite bed is due to buoyancy effects on the fuel particles that are located immersed in the dense bed, enhancing a faster heating of the biomass particles and a higher char conversion.

Sepiolite was found to be an effective primary method to reduce the tars generation directly inside the gasifier. Furthermore, a higher value of the lower heating value of the producer gas and a higher hydrogen concentration was also obtained for the same operating conditions in the sepiolite bed, which may be attributed to a higher interaction between tars and biomass char and enhanced char gasification in this lighter bed. The performance of the sepiolite bed was also analyzed in long-term tests, in which the tars generation was slightly higher, but the lower heating value of the producer gas was maintained.

Acknowledgments

This project has received funding from European Union's Horizon 2020 Research and Innovation Programme under grant agreement number 731101 (BRISK II).

References

[1] Pio D.T., Tarelho L.A.C., Matos M.A.A. Characteristics of the gas produced during biomass direct gasification in an autothermal pilot-scale bubbling fluidized bed reactor. Energy 2017; 120, 915-928.

[2] Belgiorno V., De Feo G., Della Rocca C., Napoli R.M.A., Energy from gasification of solid wastes. Waste Management 2003; 23, 1-15.

[3] Karl J., Pröll T. Steam gasification of biomass in dual fluidized bed gasifiers: A review. Renewable and Sustainable Energy Reviews 2018; 98, 64-68.

[4] Raheem A., Ji G., Memon A., Sivasangar S., Wang W., Zhao M., Hin Y. Yap T. Catalytic gasification of algal biomass for hydrogen-rich gas production: parametric optimization via central composite design. Energy Conversion and Management 2018; 158, 235-245.

[5] Zhao L., Lu Y. Hydrogen production by biomass gasification in a supercritical water fluidized bed reactor: a CFD-DEM study. Journal of Supercritical Fluids 2018; 131, 26-36.

[6] Morin M., Nitsch X., Hémati M. Interactions between char and tar during the steam gasification in a fluidized bed reactor. Fuel 2018; 224, 600-609.

[7] Devi L., Ptasinski K.J., Janssen F.J.J.G. A review of the primary measures for tar elimination in biomass gasification processes. Biomass & Bioenergy 2003; 24, 125-140.

[8] Pfeifer C., Koppatz S., Hofbauer H. Steam gasification of various feedstocks at a dual fluidised bed gasifier: Impacts of operation conditions and bed materials. Biomass Conversion & Biorefinery 2011; 1, 39-53.

[9] Gómez-Barea A., Leckner B. Modelling of biomass gasification in fluidized bed. Progress in Energy and Combustion Science 2010; 36(4), 444-509.

[10] Gómez-Barea A., Ollero P., Leckner B. Optimization of char and tar conversion in fludized bed biomass gasifiers. Fuel 2013; 103, 42-52.

[11] Mauerhofer A.M., Schmid J.C., Benedikt F., Fuchs J., Müller S., Hofbauer H. Dual fluidized bed steam gasification: Change of product gas quality along the reactor height. Energy 2019; 173, 1256-1272.

[12] Soria-Verdugo A., García-Gutiérrez L.M., Sánchez-Delgado S., Ruiz-Rivas U. Circulation of an object immersed in a bubbling fluidized bed. Chemical Engineering Science 2011; 66, 78-87.

[13] Soria-Verdugo A., García-Gutiérrez L.M., García-Hernando N., Ruiz-Rivas U. Buoyancy effects on objects moving in a bubbling fluidized bed. Chemical Engineering Science 2011; 66, 2833-2841.

[14] Soria-Verdugo A., García-Hernando N., Almendros-Ibáñez J.A., García-Hernando U. Motion of a large object in a bubbling fluidized bed with a rotating distributor. Chemical Engineering and Processing 2011; 50, 859-868.

[15] Lundberg L., Soria-Verdugo A., Pallarès D., Johansson R., Thunman H. The role of fuel mixing on char conversion in a fluidized bed. Powder Technology 2017; 316, 677-686.

[16] Sutton D., Kelleher B., Ross J.R.H. Review of literature on catalysts for biomass gasification. Fuel Processing Technology 2001; 73, 155-173.

[17] Berdugo Vilches T., Marinkovic J., Seemann M., Thunman H. Comparing active bed materials in a dual fluidized bed biomass gasifier: olivine, bauxite, quartz-sand, and ilmenite. Energy and Fuels 2016; 30, 4848-4857.

[18] Tursun Y., Xu S., Abulikemu A., Dilinuer T. Biomass gasification for hydrogen rich gas in a decoupled tripel bed gasifier with olivine and NiO/olivine. Bioresource Technology 2019; 272, 241-248.

[19] Marinkovic J., Thunman H., Knutsson P., Seemann M. Characteristics of olivine as a bed material in an indirect biomass gaisifer. Chemical Engineering Journal 2015; 279, 555-566.

[20] Devi L., Ptasinski K.J., Janssen F.J.J.G., van Paasen S.V.B., Bergman P.C.A., Kiel J.H.A. Catalytic decomposition of biomass tars: use of dolomite and untreated olivine. Renewable Energy 2005; 30(4), 565-587.

[21] Świerczyński D., Courson C., Bedel L., Kiennemann A., Vilminot S. Oxidation reduction behavior of iron-bearing olivines (Fex Mg1-x) 2SiO4 used as catalysts for biomass gasification. Chemistry of Matererials 2006; 18, 897-905.

[22] Christodoulou C., Grimekis D., Panapoulus K.D., Pachatouridou E.P., Iliopoulou E.F., Kakaras E. Comparing calcined and un-treated olivine as bed materials for tar reduction in fluidized bed gasification. Fuel Processing Technology 2014; 124, 275-585.

[23] Meng J., Wang X., Zhao Z., Zheng A., Huang Z., Wei G., Lv K., Li H. Highly abrasion resistant thermally fused olivine as in-situ catalysts for tar reduction in a circulating fluidized bed biomass gasifier. Bioresource Technology 2018; 268,212-220.

[24] Ito K., Moritomi H., Yoshie R., Uemiya S., Nishimura M. Tar capture effect of porous particles for biomass fuels under pyrolyisis conditions. Journal of Chemical Engineering of Japan 2003; 36, 840-845.

[25] Namioka T., Yoshikawa K., Hatano H., Suzuki Y. High tar reduction with porous particles for low temperature biomass gasification: effects of porous particles on tar and gas yields during sawdust pyrolysis. Journal of Chemical Engineering of Japan 2003; 36, 1440-1448.

[26] Xie Y. R., Shen L.H., Xiao J., Xie D., Zhu J. Influences of additives on steam gasification of biomass. Pyrolysis procedure. Energy and Fuels 2009; 23, 5199-5205.

[27] Noda R., Ito T., Tanaka N, Horio M. Steam gasification of cellulose and Wood in a fluidized bed of porous clay particles. Journal of Chemical Engineering of Japan 2009; 42, 90-501.

[28] Veses A., Aznar M. López M. J., Callén M. S., Murillo R., García T. Production of upgraded bio-oils by biomass catalytic pyrolysis in an auger reactor using low cost materials. Fuel 2015; 141,17-22.

[29] Serrano D., Sánchez-Delgado S., Horvat A. Effect of sepiolite bed material on gas composition and tar mitigation during C. cardunculus L. gasification. Chemical Engineering Journal 2017; 317, 1037-1046.

[30] Fuentes-Cano D., Gómez-Barea A., Nilsson S., Ollero P. Decomposition kinetics of model tar compounds over chars with different internal structure to model hot tar removal in biomass gasification. Chemical Engineering Journal 2013; 228, 1223-1233.

[31] Shen Y. Chars as carbonaceous adsorbents/catalysts for tar elimination during biomass pyrolysis or gasification. Renewable and Sustainable Energy Reviews 2015; 43, 281-295.

[32] Klinghoffer N.B., Castaldi M.J., Nzihou A. Catalyst properties and catalytic performance of char from biomass gasification. Industrial & Engineering Chemical Resources 2012; 51, 13113-13122.

[33] Hosokai S., Kumabe K., Ohshita M., Norinaga K., Li C.-Z., Hayashi J.-I. Mechanism of decomposition of aromatics over charcoal and necessary conditions for maintaining its activity. Fuel 2008; 87, 2914-2922.

[34] Zuber C., Husmann M., Schroettner H., Hochenauer C., Kienberger T. Investigation of sulfidation and regeneration of ZnO-adsorbent used in a biomass tar removal process based on catalytic steam refroming. Fuel 2015, 153, 143-153.

[35] Soria-Verdugo A., Goos E., García-Hernando N. Effect of the number of TGA curves employed on the biomass pyrolysis kinetics results obtained using the Distributed Activation Energy Model. Fuel Processing Technology 2015; 134, 360-371.

[36] Soria-Verdugo A., Goos E., García-Hernando N., Riedel U. Analyzing the pyrolysis kinetics of several microalgae species by various differential and integral isoconversional kinetic methods and the Distributed Activation Energy Model. Algal Research 2018; 32, 11-29.

[37] Gómez-Hernández J., Serrano D., Soria-Verdugo A., Sánchez-Delgado S. Agglomeration detection by pressure fluctuation analysis during Cynara

cardunculus L. gasification in a fluidized bed. Chemical Engineering Journal 2016; 284, 640-649.

[38] Anca-Couce A., Sommersacher P., Scharler R. Online experiments and modelling with a detailed reaction scheme of single particle biomass pyrolysis. Journal of Analytical and Applied Pyrolysis 2017; 127, 411-425.

[39] Caposciutti G., Almuina-Villar H., Dieguez-Alonso A., Gruber T., Kelz J., Desideri U., Hochenauer C., Scharler R., Anca-Couce A. Experimental investigation on biomass shrinking and swelling behaviour: particles pyrolysis and wood logs combustion. Biomass & Bioenergy 2019; 123, 1-13.

[40] Ku X., Jin H., Lin J. Comparison of gasification performances between raw and torrefied biomasses in an air-blown fluidized-bed gasifier. Chemical Engineering Science 2017; 168, 235-249.

[41] Anukam A., Mamphweli S., Reddy P., Meyer E., Okoh O. Pre-processing of sugarcane bagasse for gasification in a downdraft biomass gasifier system: a comprehensive review. Renewable and Sustainable Energy Reviews 2016; 66, 775-801.

[42] Olofsson G., Ye Z., Bjerle I., Andersson A. Bed agglomeration problems in fluidized bed biomass combustion. Industrial & Engineering Chemistry Research 2002; 41(2), 2888-2894.

[43] Soria-Verdugo A., Morato-Godino A., García-Gutiérrez L.M., García-Hernando N. Pyrolysis of sewage sludge in a fixed and a bubbling fluidized bed – Estimation and experimental validation of the pyrolysis time. Energy Conversion and Management 2017; 144, 235-242.

[44] Morato-Godino A., Sánchez-Delgado S., García-Hernando N., Soria-Verdugo A. Pyrolysis of Cynara cardunculus L. Samples – Effect of operating conditions and bed storage on the evolution of the conversion. Chemical Engineering Journal 2018; 351, 371-381.

[45] Geldart D. Types of gas fluidization. Powder Technology 1973; 7, 285-292.

[46] Carman P.C. Fluid flow through granular beds. Institution of Chemical Engineers 1937; 15, 150-166.

[47] Sánchez-Prieto J., Soria-Verdugo A., Briongos J.V., Santana D. The effect of temperature on the distributor design in bubbling fluidized beds. Powder Technology 2014; 261, 176-184.

[48] Serrano D., Sánchez-Delgado S., Sobrino C., Marugán-Cruz C. Defluidization and agglomeration of a fluidized bed reactor during Cynara cardunculus L. gasification using sepiolite as a bed material. Fuel Processing Technology 2015; 131, 338-347.

[49] Pathasarathy P., Narayanan K.S. Hydrogen production from steam fasification of biomass: Influence of process parameters on hydrogen yield – A review. Renewable Energy 2014; 66, 570-579.

[50] Schweitzer D., Gredinger A., Schmid M., Waizmann G., Beirow M., Sporl R., Scheffknecht G. Steam gasification of wood pellets, sewage sludge and manure: Gasification performance and concentration of impurities. Biomass & Bioenergy 2018; 111, 308-319.

[51] Kraussler M., Binder M., Schindler P., Hofbauer H. Hydrogen production within a polygeneration concept based on dual fluidized bed biomass steam gasification. Biomass & Bioenergy 2018; 111, 320-329.

[52] Basu P. Biomass Gasification and Pyrolysis – Practical Design and Theory. 1st Ed. Academic Press, 2010.

[53] Karatas H., Akgun F. Experimental results of gasification of walnut shell and pistachio shell in a bubbling fluidized bed gasifier under air and steam atmospheres. Fuel 2018; 214, 285-292.

[54] Bridgwater A.V. The technical and economic feasibility of biomass gasification for power generation. Fuel 1995; 74, 631-653.

[55] Fuentes-Cano D., Gómez-Barea A., Nilsson S., Ollero P. The influence of temperature and steam on the yields of tar and light hydrocarbon compounds during devolatilization of dried sewage sludge in a fluidized bed. Fuel 2013; 108, 341-350.

[56] Rakesh N., Dasappa S. Analysis of tar obtained from hydrogen-rich syngas generated from a fixed bed downdraft biomass gasification system. Energy Conversion and Management 2018; 167, 134-146.

List of figures

List of tables

Table 9. Producer gas composition during the long-term test in the sepiolite bed and deviation from the regular test at σ = 6 [%].

Table 10. Comparison of tars of different classes generated during the long-term and the regular tests in the sepiolite bed at σ = 6 [g/Nm^3].